sustainability

MDPI

Article

Analytical Model for the Design of HSFC and UHSFC Jackets with Various Steel Fiber Volume Fraction Ratios for the Retrofitting of RC Beam-Column Joints

Alexander-Dimitrios Tsonos and George Kalogeropoulos *

Department of Civil Engineering, Aristotle University of Thessaloniki, 54-124 Thessaloniki, Greece; tsonosa@civil.auth.gr
* Correspondence: geokal@civil.auth.gr; Tel.: +30-6953-091-705

Abstract: High-strength steel fiber-reinforced concrete (HSFC) and ultra-high strength steel fiber-reinforced concrete (UHSFC) jackets have been proved experimentally to be much more effective with respect to other strengthening schemes in improving the hysteresis performance of existing substandard reinforced concrete (RC) structural members. In this paper, an existing analytical model for the prediction of the shear capacity of RC beam-column joints strengthened with a HSFC or UHSFC jacket is extended to provide design formulation of these innovative HSFC and UHSFC jackets. An authoritative validation of the proposed formulation is also achieved by comparisons of experimental results of 50 beam-column joint specimens with the analytical predictions of the model. Test data used for verification have been collected from the literature based on experimental studies of the authors and other researchers. The merits of the HSFC and UHSFC jacketing technique are also highlighted in the state of practice. Design and application of the proposed fiber-reinforced concrete jackets in deficient existing RC beam-column joints provides a sustainable strengthening technique by contributing to the reduction in the cost and to labor-intensive procedures of common jackets by completely replacing the installation of reinforcement.

Keywords: high-strength steel fiber-reinforced concrete; ultra-high strength steel fiber-reinforced concrete; jacketing; reinforced concrete; sustainable retrofit technique; beam-column joints; hysteresis performance

check for updates

Citation: Tsonos, A.-D.; Kalogeropoulos, G. Analytical Model for the Design of HSFC and UHSFC Jackets with Various Steel Fiber Volume Fraction Ratios for the Retrofitting of RC Beam-Column Joints. *Sustainability* **2021**, *13*, 11209. https://doi.org/10.3390/su132011209

Academic Editor: Rishi Gupta

Received: 27 August 2021
Accepted: 8 October 2021
Published: 11 October 2021

1. Introduction

Earthquake events of the last sixty years worldwide revealed numerous weaknesses of reinforced concrete (RC) structures built in the 1950s–1970s period or previously [1–6]. The devastating social and economic impact caused by catastrophic collapses triggered the reformation and refinement of the building codes, while also clearly demonstrating the immense need for retrofitting of the existing RC structures. The latter are framed structures with low strength and ductility as well as poor deformation capacity. As a result, damages incurred by earthquakes are mainly concentrated in the vertical members of the bearing system and particularly in the beam-column connections, which are members with limited dimensions subjected to extreme forces [7]. Hence, the brittle response of the beam-column joints decisively affects the overall seismic performance of the existing RC structures, which show poor and degrading hysteresis behavior and, in many cases, collapse [8–16].

Both the post-earthquake and, primarily, the pre-earthquake retrofitting of existing RC buildings are critical to secure the ductile performance and preservation of structural integrity of the strengthened structures, while preventing undesirable brittle failures. Moreover, instead of demolishing and rebuilding, the earthquake-resistant rehabilitation of the existing RC structures to meet increased design earthquake demands allows for the extension of their service life. In fact, the latter can and should be achieved in a cost-effective and sustainable manner, while also protecting the environment.

The strengthening of the existing structures can be achieved using various conventional or/and innovative materials and techniques. The retrofit schemes also depend on the selected strengthening strategies. One of the most popular and suitable methods for the retrofitting of columns, walls and beam-column connections is the use of common RC jacketing with conventional steel reinforcing bars and stirrups [17–23]. This method requires increased labor work; nevertheless, it also offers some significant advantages, such as the addition of new longitudinal and transverse steel reinforcement, while also securing the confinement of the joint region [4]. The latter is not true for the fiber reinforced polymer (FRP) wrapping technique which is ineffective in confining the beam-column connections [1,24]. Shotcrete jacketing is an alternative method which can be used in the repair works and, in some cases, provides advantages over conventional concrete jacketing related to the convenience and cost [20].

It is worth noting that the strengthening of RC buildings is a difficult process which may have costs comparable to that of the usual construction works for new RC buildings. Therefore, it is crucial to consider feasibility, cost and simplicity of application for each technique when deciding on the appropriate retrofit method. This conception resulted in the introduction of a new, equally effective, simpler in application and more economical (with respect to the aforementioned) retrofit method, the fiber-reinforced concrete or shotcrete jacketing. The latter has been satisfactorily applied in many construction applications, eliminating or significantly reducing the conventional reinforcement of structures and the construction cost. Henager [25] used steel fiber-reinforced concrete (SFC) with fiber volume fraction ratio of 1.67% to replace all the hoops of the beam-column connection and part of the hoops of the critical regions of the beam and columns of a beam-column joint subassemblages, achieving a 50% reduction in the construction cost. Nevertheless, recent studies addressed that it is difficult to expect full replacement of conventional steel reinforcement by steel fibers, even using SFC with advanced mechanical properties [26–30]. The optimal solution could be found with the use of SFC in combination with RC or else concrete reinforced with an optimum amount of steel fibers and steel conventional reinforcement in a reduced ratio [27,30]. The key in this aspect is to design concrete structural members with steel fibers and reinforcing bars and stirrups with adequate safety and ductility that satisfy specific requirements. In this point of view, analysis and numerical simulation of real-scale members is of great importance to optimize the structural design. Recent studies highlighted the aspect of simulation in the performed laboratory test and appropriately approximate the specific input parameters of the SFC for nonlinear analysis [31–33].

Despite the indisputable advantages provided by using SFC [26–29,34,35], regarding the significant reduction (or elimination) of conventional steel reinforcement and lower cost, a widely accepted and reliable way of applying this material for the strengthening of the existing old RC structures is yet to be found. Infiltration of continuous steel fiber mats with specially designed cement-based slurry is a technique called SIMCON [36] which seems to be particularly effective in retrofitting processes aiming to increase shear strength and ductility of RC walls, columns and beams. However, similarly to the FRP strengthening technique, the (horizontal) wrapping layers are terminating at the floor slab level; thus, flexural strengthening of the columns cannot be achieved while the beam-column joint region still remains weak and susceptible to exhibiting severe earthquake damage. This was also demonstrated by the hysteresis behavior and failure mode of planar-type (without slab) RC beam-column joint subassemblages retrofitted using the SIMCON technique [37], which exhibited significant damage concentration in the joint region. In the experimental works of Tsonos [38,39], an innovative strengthening technique was presented for the first time, which includes the construction of high strength fiber-reinforced concrete (HSFC) or ultra-high strength fiber-reinforced concrete (UHSFC) jackets without conventional steel reinforcement or any other reinforcement technique, which ensures the satisfactory seismic performance of existing RC structures, strengthened by using composite materials. The latter new method includes the construction of a local UHSFC jacket without conventional steel reinforcement in the joint region, while the

adjacent columns are strengthened using FRPs. Both innovative strengthening techniques were found to be particularly effective in securing the ductile seismic performance of the retrofitted beam-column joint subassemblages. In all specimens the concentration of damage and the formation of plastic hinges were shifted in the beams, while the joint region and the columns remained intact. Based on this research, Tsonos holds a Patent No. 1005657 awarded by the Greek Industrial Property Organization (OBI) [40].

The design of beam-column connections to remain elastic during strong seismic events is crucial and vital not only for the new RC buildings but for the existing ones that have been retrofitted as well. However, this cannot be achieved solely by satisfying design requirements such as the flexural strength ratio value ($\Sigma M_{Rc}/\Sigma M_{Rb} > 1.30$ according to the EC8 for ductility class medium buildings). On the contrary, the determination of the developed shear stresses during cycling, which should remain low to prevent shear failure of the joint, is necessary as well [41,42]. This is possible by implementing the analytical formulation proposed by Tsonos (Tsonos model) [41–43], which allows for both the precise calculation of the actual shear stresses when yielding of the beam(s) reinforcement occurs and for the accurate prediction of the ultimate joint shear capacity. By comparing these values, the seismic behavior of the joints and the type of earthquake damages can be predicted for both the modern and the old existing buildings. Therefore, the application of the Tsonos model for the design of modern RC constructions as well as for the design of retrofit schemes for old, but also for modern structures using RC jackets, ensures the ductile seismic response of the beam-column joints.

In the present study, this internationally recognized and widely accepted analytical formulation (Tsonos model) is further extended to predict the seismic behavior of beam-column joints strengthened with HSFC or UHSFC jackets. The proposed innovative jackets include various steel fiber volume fraction ratios depending on the design strength demands, whereas conventional steel reinforcement (bars or stirrups) is not required. Consequently, the extended analytical model is a significant contribution to the satisfactory designing of innovative, reliable, easy to apply and cost-effective retrofit schemes with fiber-reinforced concrete jackets of high or ultra-high strength that secure the ductile seismic performance of the strengthened structures. For this reason, the acquired experimental results derived from the cyclic loading tests of six exterior RC beam-column joint subassemblages, strengthened using HSFC and UHSFC jackets, which were tested on previous works of Tsonos [38,39] are used. Further validation of the proposed formulation is also achieved by comparisons of the analytical predictions of the model with 44 experimental results collected from relative studies of other researchers [17,24,44–46].

2. Significance of Research

The aforementioned literature review and the findings of recent relative studies highlighted the need to ensure the long-term sustainability of real-life existing RC buildings in earthquake-prone regions. Most of them are frame RC structures with common problems such as under-reinforced beam-column joint regions, use of low strength materials, age-related deterioration, cracks and damages due to earthquake excitations and lack of the required seismic-resistant demand. Sustainable and easy-to-apply strengthening techniques in such RC frame structures are required since proper retrofitting would extend their service life, providing environmental protection and important economic gain.

Most common strengthening techniques of RC joints include the application of concrete or steel or FRP jackets. Each technique requires a different level of artful detailing and consideration of labor, cost, disruption of building occupancy and range of consideration. Obvious shortcomings of RC jackets are the required labor-intensive procedures that include perforating the slab, drilling through the existing RC structural members and the in-place installation, bending and anchoring of the reinforcing bars and stirrups. Further, such jackets significantly increase the cross-sectional dimensions of the structural members that reduces the available space and increases dynamic characteristics of the entire RC structure.

Applications of FRP materials such as jackets in beam-column joint areas have also obvious constructional limitations such as the existing slab, transverse and spandrel beams. Preparation of the concrete surface before FRP installation is a difficult and essential labor, too. Further, bond and adequate anchorage of FRP sheets and strips is a difficult task that has to be faced efficiently since premature debonding FRP failure usually occurs. This common failure mode of such composite materials causes severe and mainly unpredicted reduction in their potential strength.

These reasons make the application of HSFC or UHSFC jacketing a promising alternative strengthening technique to upgrade the shear capacity of the beam-column joint region, which requires further attention and investigation. Only a few studies, mostly carried out from the authors, deal with the use of advanced concrete jackets with steel fibers in the joint region of existing RC beam-column joint structural members. First results of these studies indicate that joint specimens strengthened with a HSFC or UHSFC jacket would be particularly useful to satisfactorily prevent brittle shear failure while securing the ductile response of the joint. In this study, crucial parameters are examined, such as the jacket width and the steel fiber volume fraction ratio that significantly affect the seismic response of the strengthened members. An analytical model is proposed for the first time for the design of innovative HSFC or UHSFC jackets, based on the experimental results of six retrofitted RC beam-column joint subassemblages which were tested in previous works of the authors. Analytical predictions of the model are also verified against test data collected from the literature.

3. Effectiveness of the Innovative HSFC and UHSFC Jackets—Experimental Results

Tsonos [38,39] examined the effectiveness of innovative SFC jackets of high and ultra-high strength in the earthquake-resistant rehabilitation of existing poorly detailed exterior RC beam-column joint subassemblages. Six original specimens (M1, M2, M3, M4, W3 and G1) of 1:2 scale, representative of structural members found in existing pre-1960s–1970s RC buildings, were designed and constructed with poor reinforcement details, flexural strength ratio lower than 1.0 and lack of ties in the joint region. Subsequently, the original specimens were strengthened with SFC jackets of ultra-high strength (specimens M1, M2, M3 and W3) and of high strength (M4 and G1), without the addition of conventional steel reinforcement. The examined variables were the width of the innovative jackets, which equaled to 40 mm, 50 mm or 60 mm, and the steel fiber volume fraction ratio, which equaled to 1.0% or 1.5%. The strengthened beam-column joints were designated UHSFM1, UHSFM2, UHSFM3, HSFM4, FHSFW3 and HSFG1, respectively. In Table 1 the details of the retrofitted specimens are summarized. All specimens were subjected to the same history of reversed inelastic lateral displacements under constant axial loading of the columns.

Table 1. Details of the strengthened beam-column joint subassemblages tested on previous works of Tsonos [38,39].

Specimen	Compressive Strength of the Jacket (MPa)	Steel Fiber Volume Fraction Ratio (%)	Thickness of the Jacket (mm)	Strengthened Structural Members
UHSFM1	106.33	1.5	40	B/C Joint and Columns: with UHSF concrete jacket
UHSFM2	106.33	1.5	60	
UMSFM3	102.3	1.0	60	
HSFM4	65	1.5	60	B/C Joint and Columns: with HSF concrete jacket
FHSFW3	106.33	1.5	50	B/C Joint: with local UHSF concrete jacket; Columns: with FRP-wrapping
HSFG1	60	1.0	60	B/C Joint and Columns: with HSF concrete jacket

In the following, a comprehensive interpretation of the seismic behavior is performed to evaluate the hysteresis response of subassemblages UHSFM1, UHSFM2, UHSFM3, HSFM4, FHSFW3 and HSFG1, based on the experimental data acquired during testing. This analysis is critical as it enables to deeply understand the developed failure mechanisms, while also allows the further exploitation of the experimental results to check the accuracy

of the proposed analytical model in predicting the seismic behavior of the strengthened specimens with the HSFC and UHSFC jackets.

3.1. Seismic Response of the Jacketed Subassemblages

The retrofitted beam-column joint specimens UHSFM1, UHSFM2, UHSFM3, HSFM4, FHSFW3 and HSFG1 exhibited a ductile hysteresis behavior characterized by the complete absence of damage in the joint region and the adjacent columns. The innovative HSFC and UHSFC jackets provided substantial improvement in the lateral bearing capacity, peak-to-peak stiffness, energy dissipation capacity and ductility of the enhanced specimens with respect to the corresponding original ones, M1, M2, M3, M4, W3 and G1. Moreover, the concentration of damage was satisfactorily shifted in the beam of the strengthened specimens where the plastic hinges were formed. As a result, the application of the innovative HSFC or UHSFC jacket allowed the complete transformation of the hysteresis performance of the original subassemblages, which was dominated by brittle shear failure of the joint region, to the ductile flexural response of the strengthened specimens. The latter is also clearly reflected in the envelope curves of the hysteresis loops of the strengthened subassemblages, illustrated in Figure 1. As it can be observed, the retrofitted specimens showed stable (push half-cycles) or increasing (pull half-cycles) lateral bearing capacity, owed to the increased inherent strength of the steel fiber jackets. A minor reduction in lateral strength occurred for drift angle, R, values greater than 4.21%. Nevertheless, at the end of testing, specimens UHSFM1, UHSFM2, UHSFM3, HSFM4, FHSFW3 and HSFG1 maintained 68.82%, 88.71%, 79.08%, 66.25%, 81.81% and 86.67% (push half-cycles) and 103%, 63.3%, 97.87%, 94.33%, 109% and 99.67% (pull half-cycles), respectively, of their initial lateral bearing capacity during the first cycle of the earthquake-type loading. It should be noted that the remarkably increased lateral strength of the retrofitted subassemblages was achieved without adding new conventional steel reinforcement and is exclusively attributed to the SFC jacket.

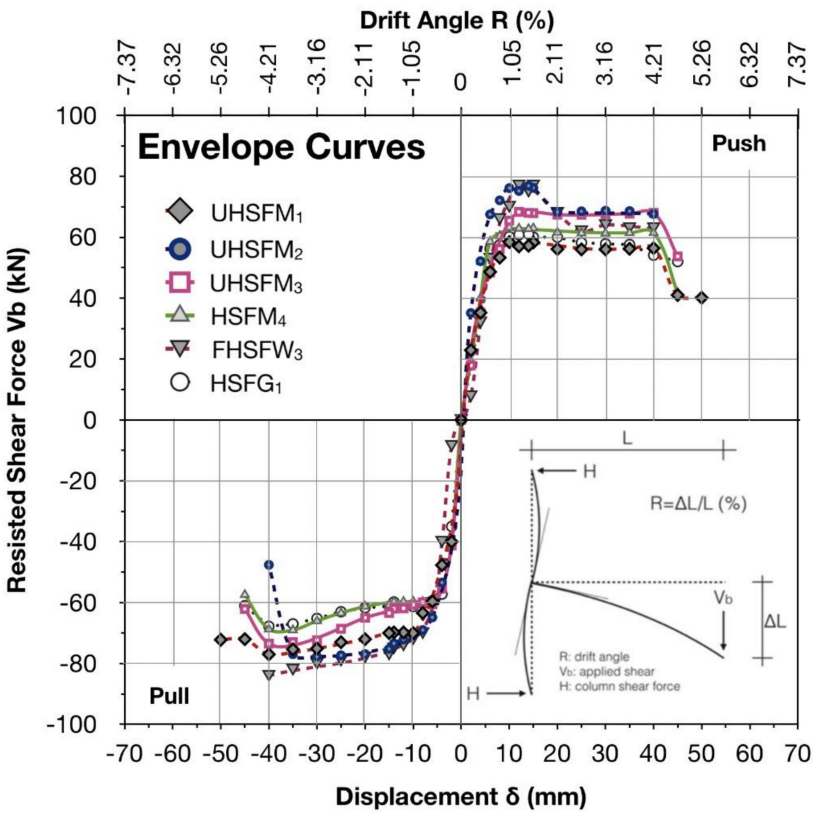

Figure 1. Envelope curves of the hysteresis loops of subassemblages UHSFM1, UHSFM2, UHSFM3, HSFM4, FHSFW3 and HSFG1 tested on previous works [38,39].

3.2. Energy Dissipation Capacity and Viscous Damping

The effectiveness of both innovative retrofit schemes, which include the use of HSFC and UHSFC jackets, is further substantiated by the experimental results regarding the energy dissipation capacity of the strengthened subassemblages. All specimens exhibited a ductile dissipating hysteresis behavior which was reflected by spindle-shaped hysteresis loops without pinching around the axes [38,39]. It is noteworthy that the amount of seismic energy dissipated in the plastic hinges formed in the beams of the retrofitted beam-column joint subassemblages, UHSFM1, UHSFM2, UHSFM3, HSFM4, FHSFW3 and HSFG1, showed a significant and continuous increase during consecutive cycles of the earthquake-type loading (see Figure 2a). This indicates an absence of shear damage in the joint region which is favorable for bond conditions between steel bars and concrete and hence allows the yielding of the beam longitudinal reinforcement and overstrength development. In the plots of energy dissipation capacity versus load point displacement, shown in Figure 2a, an increase of 246.84%, 255.85%, 285.12%, 223.93%, 307.28% and 249% in the dissipated energy value at the end of the testing with respect to the corresponding value during the first cycle of loading for specimens UHSFM1, UHSFM2, UHSFM3, HSFM4, FHSFW3 and HSFG1, respectively, was observed.

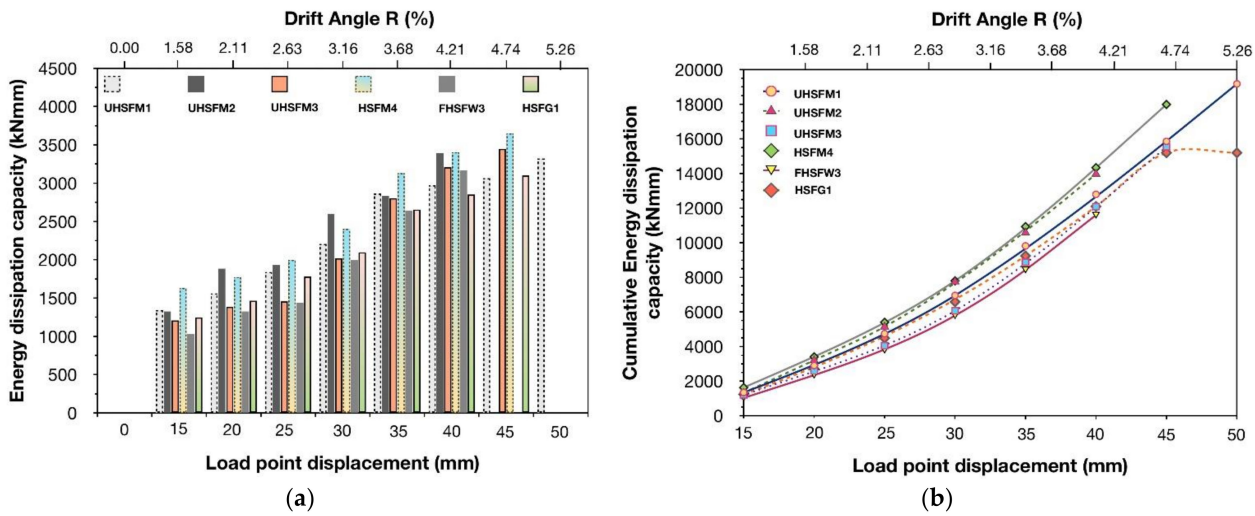

Figure 2. (**a**) Energy dissipation capacity and (**b**) cumulative energy dissipation capacity of the beam-column joint subassemblages tested by Tsonos [38,39].

The cumulative dissipated hysteretic energy of the subassemblages is depicted in Figure 2b. It was clearly demonstrated that the retrofitted specimens dissipated an immense amount of seismic energy through damping in the plastic hinges formed at the beam while the joint region remained elastic during cycling. This is owed to the increased deformability and displacement ductility provided by the innovative HSFC and UHSFC jackets. Thus, another crucial parameter for the seismic performance of the strengthened subassemblages, the equivalent viscous damping coefficient, ζ_{eq}, is subsequently examined. The latter consists of both the hysteretic and the elastic damping, while relating to the inelastic characteristics and the deformation capacity of the strengthened members. In particular, ζ_{eq} is expressed as the ratio of the dissipated seismic energy within a given cycle of the earthquake-type loading to the elastic strain energy corresponding to this cycle (see Figure 3a). Furthermore, the values of ζ_{eq} are higher for structural members which show dissipating hysteresis response. On the contrary, poor and rapidly degrading hysteresis behavior is related to possible collapse due to cumulative seismic energy under small deformations. In Figure 3a,b, the values of the equivalent viscous damping coefficient per cycle of loading and the values of cumulative equivalent viscous damping coefficient are presented. All specimens showed high values of ζ_{eq} due to their increased energy dissipation capacity.

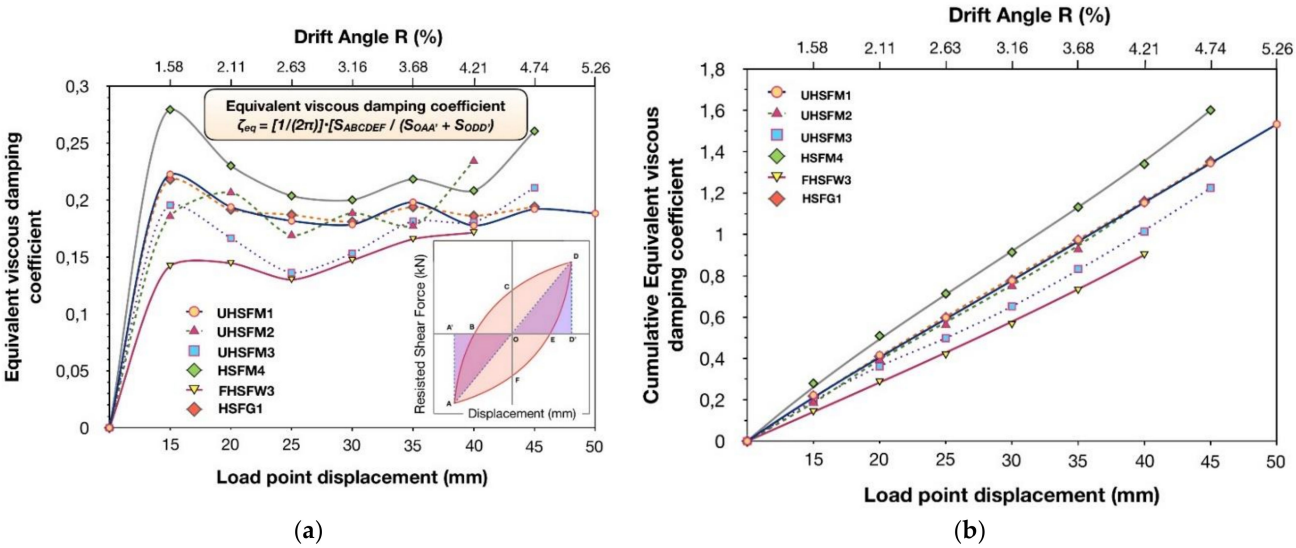

(**a**) (**b**)

Figure 3. (**a**) Equivalent viscous damping coefficient and (**b**) cumulative equivalent viscous damping coefficient of the beam-column joint subassemblages tested by Tsonos [38,39].

4. Theoretical Considerations

4.1. Tsonos Model

Non-ductile RC framed structures, designed for gravity loads only, are extremely vulnerable and susceptible to developing brittle failure mechanisms related to catastrophic (partial or general) collapse. In particular, the damages incurred by earthquakes are mostly located in the vertical members of the bearing system, namely the columns and (primarily) the beam-column joints. Moreover, the beam-column connections used to be poorly confined or even totally unconfined. As a result, the cyclic response of the joints found in existing pre-1960s–1970s RC structures is dominated by brittle shear failure, given that well-anchorage of the beam longitudinal reinforcement is provided.

Recently, in [41,42], it was clearly demonstrated both experimentally and analytically that, even in modern RC structures designed according to the recommendations of the EC8 for ductility class medium (DCM), a mixed-type failure which includes shear damage in the beam-column joint region cannot always be effectively precluded. Contrarily, if the shear stresses developed in the joint region during an earthquake event are moderate to high ($0.5\gamma_{ult} < \gamma < \gamma_{ult}$) or high ($\gamma \geq \gamma_{ult}$), the joint shear failure is possible to occur regardless of the capacity design ratio value and the number of ties provided in the joint region.

Designing the beam-column connections to remain elastic during cycling is crucial for preserving the structural integrity and preventing collapse. Thus, an analytical formulation, which allows the accurate prediction of the behavior of the beam-column joints under reversed inelastic lateral displacements, would be particularly useful to secure the desirable ductile seismic performance of the joints. Under these lines, an analytical model was proposed by Tsonos [41–43] which precisely predicts the ultimate shear capacity of the joint region, τ_{ult}, as well as the developed actual shear stress, τ_{cal}. The accuracy of the analytical formulation (Tsonos model) has been checked using data acquired from more than 160 seismic tests performed in the Laboratory of Reinforced Concrete and Masonry Structures of the Aristotle University of Thessaloniki, as well as data from numerous experimental works found in the literature. Moreover, the model is widely accepted by the scientific community and has been used to control the accuracy of other analytical models [11,47–51]. Recently [43], a more simplified version of the analytical formulation was proposed by Tsonos, while the Tsonos model was incorporated in the Final Draft EN 1998-1-2 NEN SC 8, PT 2, CEN/TC 250/SC 8 N 870 "Eurocode 8: Earthquake Resistant Design of Structures".

4.2. Analytical Formulation and Aspects of the Proposed Model

In the present study, an extension of the analytical formulation (Tsonos model) is presented for the first time, which allows for the prediction of the seismic behavior of beam-column joints strengthened with HSFRC or UHSFRC jackets with various steel fiber volume fraction ratios. The model is subsequently presented in detail and its accuracy is checked against the experimental data presented herein. It is worth noting that both SFC jackets are proved to be innovative strengthening schemes that are easy to apply while requiring no additional steel reinforcement.

In Figure 4a,b, an RC exterior and an RC interior beam-column joint of a moment resisting frame are illustrated, respectively. During earthquake excitations the developed internal shear forces in the joint core (see Figure 5) are resisted by two mechanisms. The first one is the concrete compression strut acting between diagonally opposite corners of the joint (see Figure 4c) and the second one (truss mechanism) is formed by the horizontal and the vertical reinforcement of the joint core and the concrete compression struts (see Figure 4d). The horizontal reinforcement of the beam-column connection consists of the hoops provided in the joint core, while the column's longitudinal reinforcing bars between the column's corner bars are considered the vertical reinforcement of the joint.

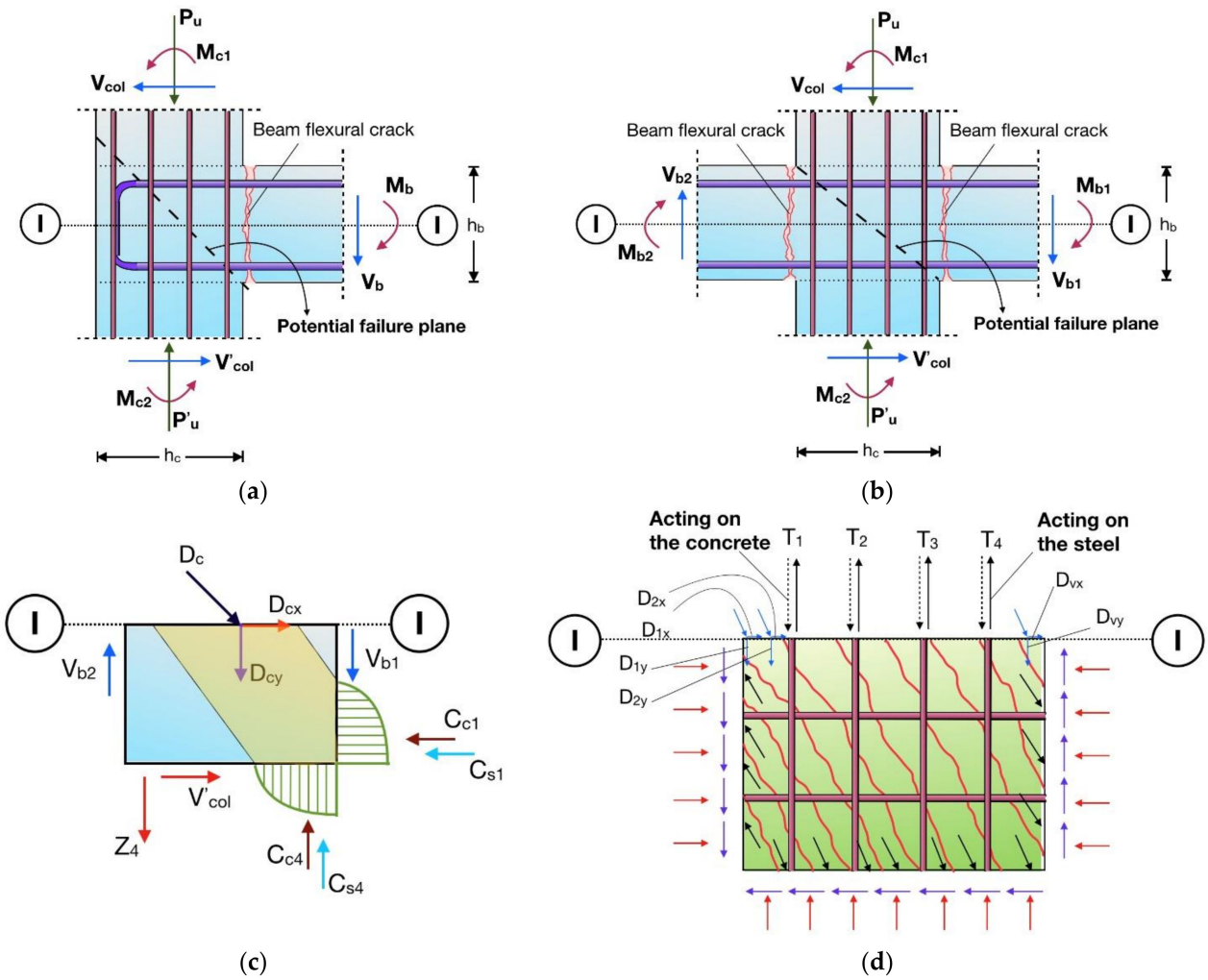

Figure 4. (**a**) Exterior beam-column joint, (**b**) interior beam-column joint, (**c**) concrete compression strut mechanism, (**d**) truss mechanism.

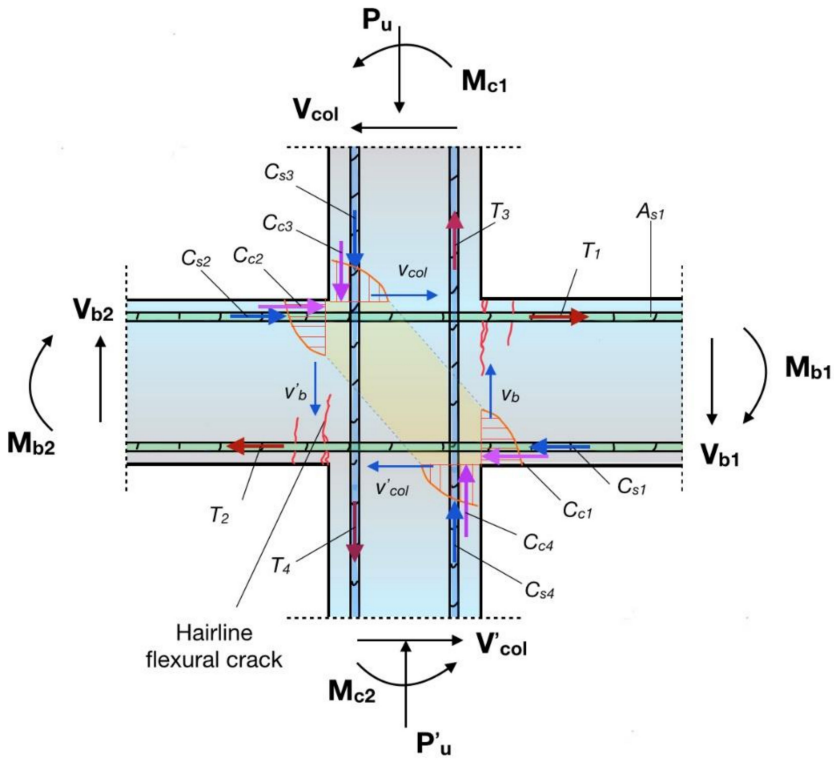

Figure 5. Forces developed in an interior RC beam-column joint due to seismic actions.

It is known that the compression strength of concrete in the joint core, that is subjected to tension and compression stress, affects both mechanisms and hence controls the ultimate strength of the joint. The latter is limited by the gradual crushing along the cross-diagonal cracks and especially along the potential failure planes (see Figure 4a,b).

In the middle of the joint height, where the flexural moment is negligible, the section I-I is considered. The forces acting in the joint core are analyzed into two components along the X and Y axes. The tensile forces, T_i, acting on the steel bars which consist of the joint vertical reinforcement, equal the opposing compression forces acting in the joint core concrete. The latter are the vertical components of the diagonal compression forces from the truss mechanism, $D_1, D_2, \ldots, D_v$ (Equation (1)).

$$D_{1y} + D_{2y} + \ldots + D_{vy} = \Sigma T_i = T_1 + T_2 + T_3 + T_4 \quad (1)$$

The axial load of the column is resisted by the compression strut mechanism. The vertical and the horizontal components of the joint shear force, V_{jv} and V_{jh}, respectively, are calculated:

$$D_{cy} + (T_1 + \ldots + T_4) = D_{cy} + D_{sy} = V_{jv} \quad (2)$$

$$D_{cx} + (D_{1x} + \ldots + D_{vx}) = D_{cx} + D_{sx} = V_{jh} \quad (3)$$

Considering that the normal stress, σ, and the shear stress, τ, are uniformly distributed over section I-I, Equations (4) and (5) are used, where h'_c and b'_c are the length and the width of the joint core.

$$\sigma = \frac{D_{cy} + D_{sy}}{h'_c \cdot b'_c} = \frac{V_{jv}}{h'_c \cdot b'_c} \quad (4)$$

$$\tau = \frac{V_{jh}}{h'_c \cdot b'_c} \quad (5)$$

A relationship between the average normal compressive stress, σ and the average shear stress, τ, is established (see Figure 6). Thus, from Equations (4) and (5):

$$\sigma = \frac{V_{jv}}{V_{jh}} = \tau \tag{6}$$

However, it has been shown [8,52,53] that:

$$\frac{V_{jv}}{V_{jh}} = \frac{h_b}{h_c} = a \tag{7}$$

where a is the joint aspect ratio.

The principal stresses σ_I and σ_{II} are calculated:

$$\sigma_{I,II} = \frac{\sigma}{2} \pm \frac{\sigma}{2} \cdot \sqrt{1 + \frac{4\tau^2}{\sigma^2}} \tag{8}$$

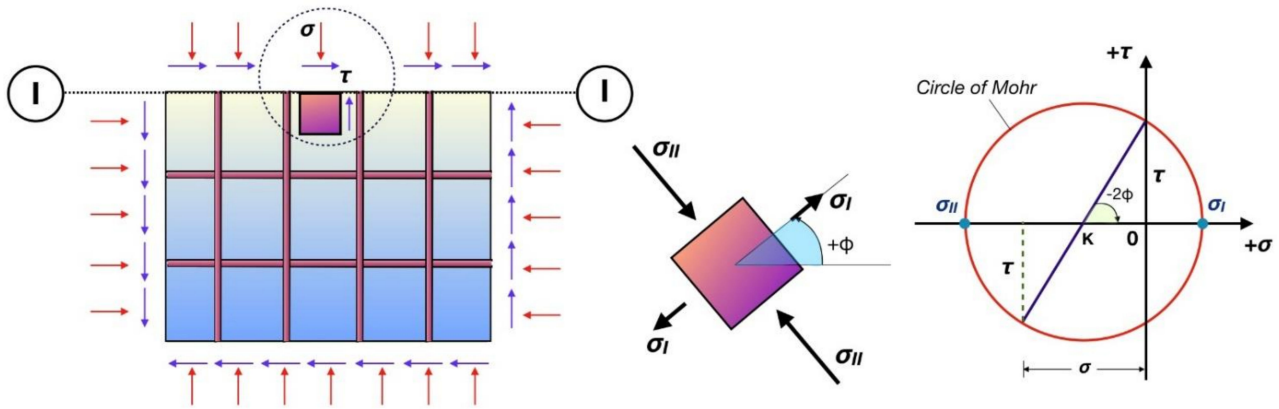

Figure 6. Element of stress state in the beam-column joint region.

In order to represent the concrete biaxial strength curve, Equation (9) of a fifth-degree parabola was used by Tsonos [41]. In Equation (10), f_c is the increased value of the concrete compressive strength due to the confinement provided to the joint core by the joint hoop reinforcement or due to the strengthening material in the case of retrofitted beam-column connections. To calculate f_c the model of Scott et al. [54] is used (Equation (11)), where f'_c is the concrete compressive strength and k is the coefficient of the model of Scott et al.:

$$-10 \cdot \frac{\sigma_I}{f_c} + \left(\frac{\sigma_{II}}{f_c}\right)^5 = 1 \tag{9}$$

$$f_c = k \cdot f'_c \tag{10}$$

$$k = 1 + \frac{\rho_s \cdot f_{yh}}{f'_c} \tag{11}$$

In Equation (11), ρ_s is the volume ratio of the transverse reinforcement and f_{yh} is its yield strength.

From Equations (6)–(9) and for $\tau = \gamma \cdot \sqrt{f_c}$ the following expression is used (Equation (12)) to represent the fifth-degree parabola.

$$\left[\frac{\alpha\gamma}{2\sqrt{f_c}}\left(1 + \sqrt{1 + \frac{4}{\alpha^2}}\right)\right]^5 + \frac{5\alpha\gamma}{\sqrt{f_c}}\left(\sqrt{1 + \frac{4}{\alpha^2}} - 1\right) = 1 \tag{12}$$

Assuming that:

$$x = \frac{\alpha\gamma}{2\sqrt{f_c}} \tag{13}$$

and

$$\psi = \frac{\alpha\gamma}{2\sqrt{f_c}}\sqrt{1+\frac{4}{\alpha^2}} \tag{14}$$

Then Equation (12) transforms into:

$$(x+\psi)^5 + 10\psi - 10x = 1 \tag{15}$$

Recently, Tsonos [43] substituted Equation (15) with a line equation which further facilitates the implementation of the analytical formulation. The latter was achieved by solving the system of Equations (13)–(15) for a wide range of joint aspect ratio values. For each value of the joint aspect ratio, the solutions of the system, x and ψ, were used to calculate the expressions $x+\psi$ and $x-\psi$.

Using the expressions:

$$\frac{\sigma_I}{f_c} = \frac{\alpha\gamma}{2\sqrt{f_c}} - \frac{\alpha\gamma}{2\sqrt{f_c}}\sqrt{1+\frac{4}{\alpha^2}} \tag{16}$$

$$\frac{\sigma_{II}}{f_c} = \frac{\alpha\gamma}{2\sqrt{f_c}} + \frac{\alpha\gamma}{2\sqrt{f_c}}\sqrt{1+\frac{4}{\alpha^2}} \tag{17}$$

and substituting (Equations (13) and (14)) to Equations (16) and (17). The following expressions are calculated (Equations (18) and (19)):

$$\frac{\sigma_I}{f_c} = x - \psi \tag{18}$$

$$\frac{\sigma_{II}}{f_c} = x + \psi \tag{19}$$

Thus, each couple of values $(x+\psi, x-\psi)$ represents a point of the concrete biaxial strength curve according to Equation (15).

In this equation, for values of $x+\psi \leq 0.55$, which correspond to aspect ratio values lower than 2.0 (as in real practice), the value $(x+\psi)^5$ in Equation (15) is quite small $(x+\psi)^5 \leq 0.051 = 5\%$ and can be ignored without affecting the curve morphology. Therefore, the curve of the concrete biaxial strength for the part BC can be simplified and substituted by a line equation (Equation (20)) (see Figure 7), which is used to calculate the ultimate shear capacity of the joint region, τ_{ult}.

$$x - \psi = -0.1 \tag{20}$$

The ultimate shear strength of the beam-column connection, τ_{ult}, depends both on the concrete compressive strength of the joint region, f_c and on the joint aspect ratio, α and is calculated by solving the system of Equations (13), (14) and (20). The developed shear stress in the joint region, calculated from the horizontal joint shear force assuming that yielding of the top beam reinforcement occurs, is expressed as $\tau_{cal} = \gamma_{cal}\sqrt{f_c}$ $(in\ MPa)$. According to the analytical formulation, the predicted actual value of the joint's shear stress, τ_{pred}, is expected to be near τ_{ult} if the calculated joint shear stress, τ_{cal}, equals or exceeds the ultimate strength, τ_{ult}, $(\tau_{cal} \geq \tau_{ult})$, because the joint fails before yielding of the beam's reinforcement is achieved. Otherwise, if the calculated joint shear stress, τ_{cal}, is lower than the ultimate strength of the connection $(\tau_{cal} < \tau_{ult})$, then the predicted actual value of the joint's shear stress, τ_{pred}, is expected to be near τ_{cal}, since the joint permits yielding of the beam reinforcement. Moreover, if the calculated joint shear stress, τ_{cal}, is lower than half the value of the ultimate strength, τ_{ult}, $(\tau_{cal} < 0.5{\cdot}\tau_{ult})$, all seismic damage

and the formation of the plastic hinges are concentrated in the adjacent beam(s), while the joint region remains intact.

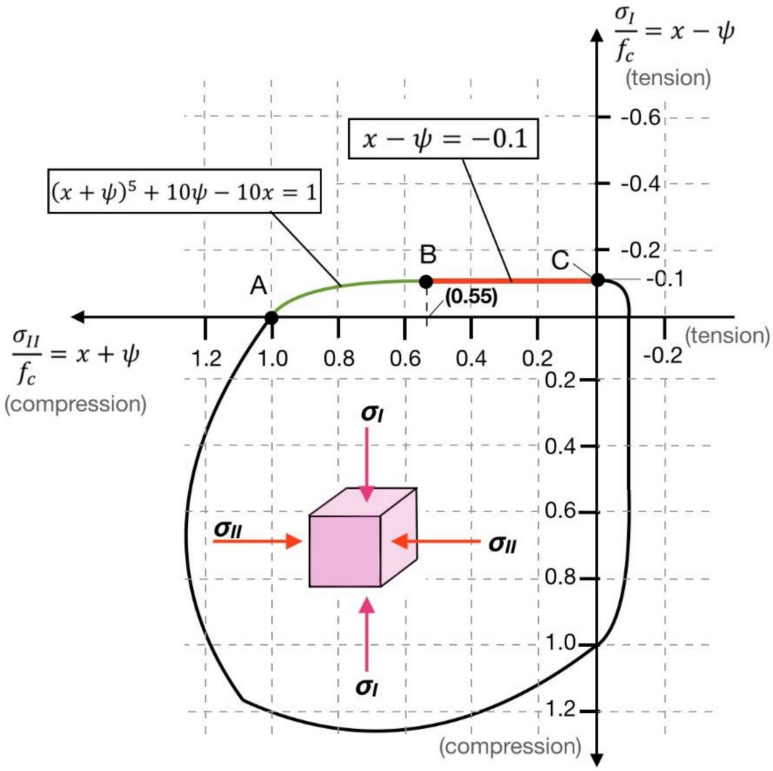

Figure 7. Biaxial concrete strength curve. For combined compression–tension stress state a fifth-degree parabola was used by Tsonos [41] to represent the biaxial concrete strength curve (part AC). The curve is further simplified for its part BC and substituted by a line equation [43].

4.3. Proposed Approach for the Design of HSFC and UHSFC Jackets

Although the increased concrete compressive strength is related to a more brittle behavior, the addition of steel fibers to the mix of high or ultra-high strength concrete allows for the exploitation of the advantages of both combined materials. Thus, a new material is created with substantially improved mechanical properties. However, the application of such an innovative material by the construction industry requires deep understanding of its behavior under biaxial loading. Based on the experimental results mentioned in Section 3 of the present study, which indisputably demonstrated the effectiveness of HSFC and UHSFC jacketing of beam-column joints, the analytical model is further extended herein to allow for the reliable analysis and design of HSFC and UHSFC jackets for the retrofitting of existing RC structures without the use of conventional reinforcement.

For joint aspect ratio values lower than 2.0, a line equation can also be used to determine the ultimate shear stress, τ_{ult}, of beam-column joints strengthened by a SFC jacket of high strength or ultra-high strength. However, in this case the line equation depends on the steel fiber volume fraction ratio. Thus, for each value of the steel fiber volume fraction ratio, the corresponding line equation which is used to calculate τ_{ult} should be determined. Based on the related literature [55–67], a coefficient, m, should be adopted for properly modifying Equation (20) to calculate the ultimate shear stress when using HSFC or UHSFC with fiber volume fraction ratio equal to 1.0% or 1.5% (Equation (21)). Kölle [59] experimentally investigated the biaxial strength of high performance SFC for different fiber types and for different fiber volume fraction ratios. He concluded that the failure envelopes for different steel fiber volume fraction ratios (1% and 2%) showed minor variations with respect to the failure envelope curve for plain high-performance concrete in the tension–compression region. The latter, however, is not true for the biaxial compression–

compression region. Moreover, the addition of steel fibers was found to increase the biaxial strength. Lee et al. [65] also experimentally investigated the biaxial strength of plain concrete of ultra-high strength and of SFC of ultra-high strength and concluded that the biaxial failure criteria of UHPFRC seem to be similar to those of normal-strength concrete, following the Kupfer's failure criteria [66]. Along these lines, the proposed values of coefficient m were approximately determined to be equal to m = 0.6 for plain concrete of high or ultra-high strength (Equation (22)); $m = 0.7$ for HSFC or UHSFC with steel fiber volume fraction ratio of 1.0% (Equation (23)); and m = 0.8 for HSFC or UHSFC with steel fiber volume fraction ratio of 1.5% (Equation (24)) (Figure 8).

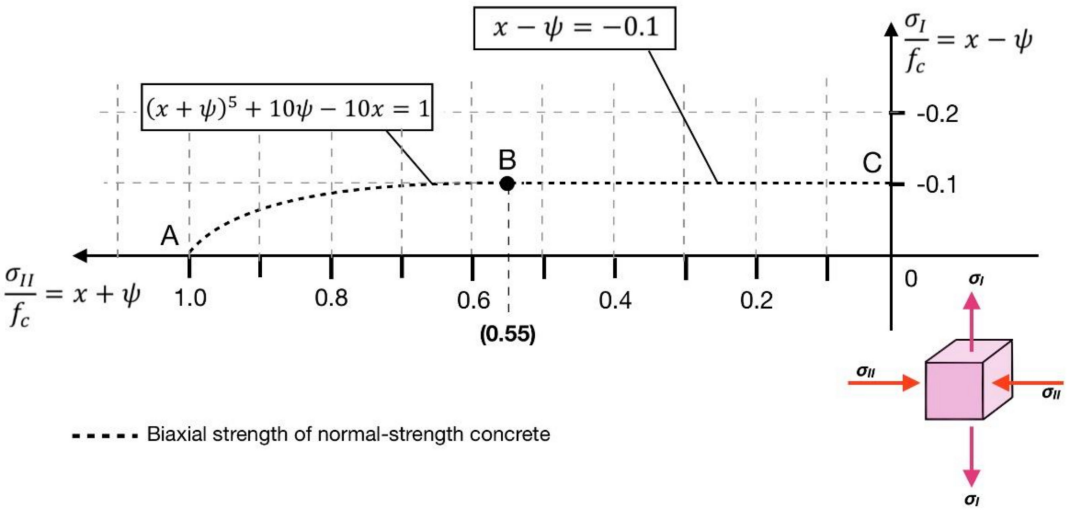

(**a**)

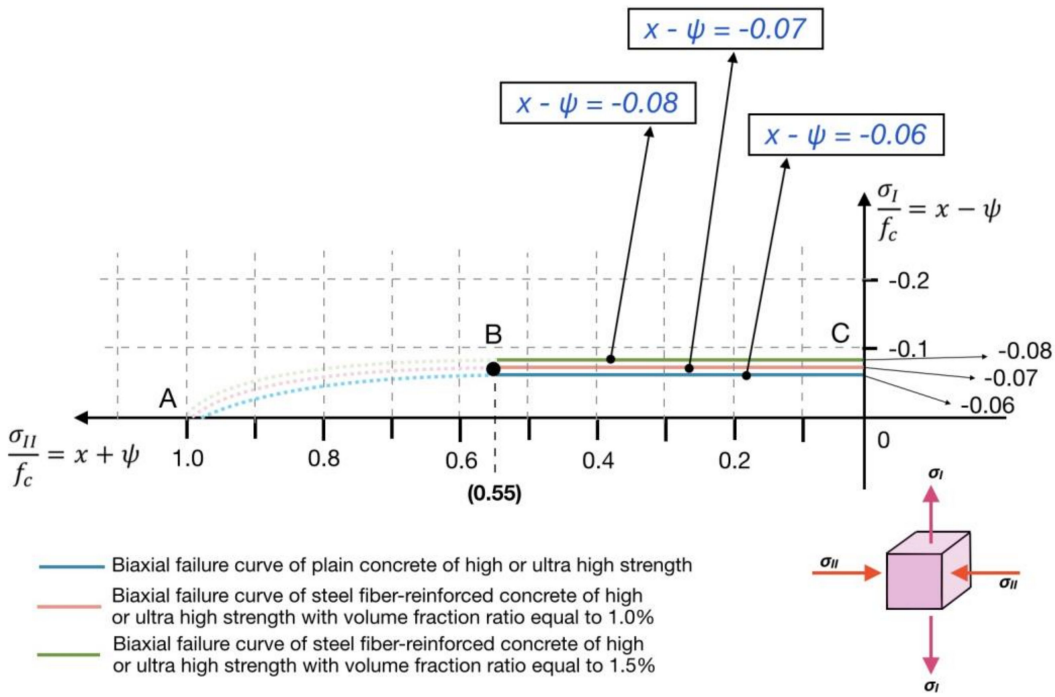

(**b**)

Figure 8. Proposed analytical formulation: (**a**) for the biaxial strength of normal-strength concrete, (**b**) for the biaxial strength of plain concrete of high and ultra-high strength and for the biaxial strength of fiber-reinforced concrete of high and ultra-high strength with steel fiber volume fraction ratio equal to 1.0% and 1.5%.

5. Verification of the Proposed Model Using Experimental Data from the Literature

5.1. Comparisons with Test Data of Tsonos

In Table 2, the ultimate strength ratios τ_{cal}/τ_{ult} and the predicted values of shear stress in the potential failure plane are calculated according to the proposed shear strength formulation for specimens UHSFM1, UHSFM2, UHSFM3, HSFM4, FHSFW3 and HSFG1 [38,39]. As can be observed, the predicted shear values verified the experimental results in all cases of the strengthened subassemblages. Furthermore, the extended form of the analytical formulation was particularly satisfactory in predicting the failure mode of UHSFM1, UHSFM2, UHSFM3, HSFM4, FHSFW3 and HSFG1, which in all cases included the concentration of damage and the formation of plastic hinges solely in the beam of the specimens, while the joint region and the columns remained intact. This was fully justified by the low actual shear stress values in the joint region which were lower than half the ultimate joint shear capacity ($\tau_{cal} < 0.5 \cdot \tau_{ult}$).

$$x - \psi = m(-0.1) \tag{21}$$

$$x - \psi = 0.6(-0.1) = -0.06 \tag{22}$$

$$x - \psi = 0.7(-0.1) = -0.07 \tag{23}$$

$$x - \psi = 0.8(-0.1) = -0.08 \tag{24}$$

Table 2. Ultimate strength ratios and predicted values of concrete shear stress in the potential failure plane.

Specimen	f_c (MPa)	γ_{cal}	γ_{ult}	τ_{cal} (MPa)	τ_{ult} (MPa)	τ_{Pred}	τ_{cal}/τ_{ult}
UHSFM1	106.33	0.31	1.38	3.20	14.23	3.20	0.22
UHSFM2	106.33	0.24	1.29	2.47	13.30	2.47	0.19
UHSFM3	102.3	0.25	1.13	2.53	11.43	2.53	0.22
HSFM4	65	0.24	1.01	1.93	8.14	1.93	0.24
FHSFW3	106.33	0.28	1.36	2.89	14.02	2.89	0.21
HSFG1	60	0.24	0.85	1.86	6.58	0.24	0.28

5.2. Comparisons with Test Data of Other Authors

The proposed analytical model has been applied to 44 beam-column joints under cyclic loading deformations in order to establish the validity of the proposed model based on a broad range of parametric studies. The database of experimental information was compiled from five existing works of literature [17,24,44–46]. Table 3 presents the main geometrical, mechanical and reinforcement characteristics of the beam-column joint specimens, the experimentally measured shear strength and the predicted one as calculated from the formulation of the model. Specifically, Table 3 includes the values of the following variables: b_c and h_c are the width and heigh of the column, respectively (see also Figure 4 for notation); b_b and h_b are the width and height (total depth) of the beam, respectively (see also Figure 4 for notation); ρ_{lc} and ρ_{lb} are the steel reinforcement ratios of the column and the beam, respectively; $\rho_{sh,j}$ and $\rho_{sv,j}$ are the horizontal and the vertical steel reinforcement ratios in the joint area, respectively; $V_{jh,exp}$ and $V_{jh,pred}$ are the experimental and the analytical shear strength of the joint, respectively, and $V_{jh,Ratio} = V_{jh,exp}/V_{jh,pred}$.

Comparisons between the test data and the analytical results shown in Table 3 clearly indicate that the proposed formulation achieves to predict with satisfactory accuracy the shear strength of the joint. Especially, the ratios of the experimental to the analytical shear strength values of 44 specimens have an average value of 0.91 and standard deviation 12%.

Table 3. Validation of the proposed model with experimental data.

Specimen Code Name	b_c (mm)	h_c (mm)	$\rho_{l,c}$ (%)	h_b (mm)	b_b (mm)	$\rho_{l,b}$ (%)	$\rho_{sh,j}$ (%)	$\rho_{sv,j}$ (%)	$V_{jh,exp}$ (kN)	$V_{jh,pred}$ (kN)	$V_{jh,Ratio}$ (exp/pred.)
A0[17]	200	200	0.79	200	300	0.26	-	-	82.94	97.69	0.85
A1[17]	200	200	0.79	200	300	0.26	0.97	-	83.27	97.69	0.85
A2[17]	200	200	0.79	200	300	0.26	1.94	-	83.27	97.69	0.85
A3[17]	200	200	0.79	200	300	0.26	2.92	-	82.62	97.69	0.85
B0[17]	200	300	0.52	200	300	0.26	-	-	244.46	248.49	0.98
B1[17]	200	300	0.52	200	300	0.70	1.94	-	247.86	257.93	0.96
C0[17]	200	300	1.29	200	300	0.75	-	0.26	243.00	248.49	0.98
C2[17]	200	300	1.29	200	300	0.75	1.94	-	247.86	267.36	0.93
C3[17]	200	300	1.29	200	300	0.75	2.92	-	243.00	276.79	0.88
C5[17]	200	300	1.29	200	300	0.75	4.86	-	252.72	279.24	0.91
4a[44]	300	300	0.89	250	500	0.79	-	-	231.27	426.97	0.54
4b[44]	300	300	0.89	250	500	0.79	-	-	270.47	426.97	0.63
4c[44]	300	300	0.89	250	500	0.79	-	-	333.19	426.97	0.78
4d[44]	300	300	3.57	250	500	0.79	-	-	293.99	426.97	0.69
4e[44]	300	300	3.57	250	500	0.79	-	-	313.59	426.97	0.73
4f[44]	300	300	3.57	250	500	0.79	-	-	358.89	426.97	0.84
5a[44]	300	300	2.18	250	500	0.79	0.54	-	455.89	460.18	0.99
5b[44]	300	300	2.18	250	500	0.79	0.54	-	477.18	460.18	1.04
5c[44]	300	300	2.18	250	500	0.79	0.54	-	474.18	460.18	1.03
5d[44]	300	300	2.18	250	500	1.29	0.54	-	454.57	633.44	0.72
5e[44]	300	300	2.18	250	500	1.29	0.54	-	593.93	633.44	0.94
5f[44]	300	300	2.18	250	500	1.29	0.54	-	647.67	633.44	1.02
A1[24]	200	200	0.79	200	300	0.26	-	-	77.76	96.70	0.80
A1[24]	200	200	0.79	200	300	0.26	-	-	79.38	96.70	0.82
B1[24]	200	200	1.70	200	300	0.26	0.67	-	79.70	96.70	0.82
B2[24]	200	200	1.70	200	300	0.26	0.67	-	79.70	96.70	0.82
3[45]	220	220	4.02	160	220	1.76	0.48	-	214.41	212.48	1.01
4[45]	220	220	4.02	160	220	1.76	0.12	-	217.80	212.48	1.03
5[45]	220	220	4.02	160	220	1.76	0.12	-	203.28	212.48	0.96
6[45]	220	220	4.02	160	220	1.76	0.12	-	213.44	212.48	1.00
9[45]	220	220	4.04	160	220	1.76	0.48	-	212.96	212.48	1.00
11[45]	220	220	4.04	160	220	1.76	0.12	-	220.22	212.48	1.04
12[45]	220	220	4.04	160	220	1.76	0.12	-	212.96	212.48	1.00
13[45]	220	220	4.04	160	220	1.76	0.48	-	216.35	212.48	1.02
14[45]	220	220	4.04	160	220	1.76	0.12	-	214.90	212.48	1.01
15[45]	220	220	4.04	160	220	1.76	0.12	-	199.41	212.48	0.94
Sp1[46]	380	380	4.24	304	508	1.25	-	-	623.81	709.31	0.88
Sp2[46]	380	380	4.24	304	508	1.25	-	-	620.92	713.34	0.87
Sp3[46]	380	380	4.24	304	508	1.25	0.09	-	658.46	715.35	0.92
Sp4[46]	380	380	4.24	304	508	1.25	0.16	-	749.44	713.34	1.05
Sp5[46]	380	380	4.24	380	508	1.00	-	-	612.26	709.31	0.86
Sp6[46]	380	380	4.24	380	508	1.00	0.28	-	745.10	719.38	1.04
Sp7[46]	380	380	4.24	380	508	1.00	0.16	-	711.89	719.38	0.99
Sp8[46]	380	380	4.24	380	508	1.34	0.28	-	854.85	766.74	1.11

6. Conclusions

The following conclusions are drawn based on the above analysis:

1. The analytical formulation (Tsonos model) is extended to allow, for the first time, the reliable analysis and design of innovative SFC jackets of high or ultra-high strength (HSFC or UHSFC) and with a volume fraction ratio equal to 1.0% or 1.5% for the retrofitting of existing RC structures.
2. Based on the experimental results found in the related literature, an approximate coefficient for modifying the equation that gives the ultimate shear capacity of the beam-column joint region was determined. In particular, three different values of the coefficient were used to determine three equations that represent the failure criteria for plain concrete of high or ultra-high strength, for SFC of high or ultra-high strength with a fraction ratio of 1.0% and for SFC of high or ultra-high strength with a fraction ratio of 1.5%.
3. The approximation of the coefficient values was made considering that the failure envelopes for different steel fiber volume fraction ratios show minor variations with respect to the failure envelope curve for plain high-performance concrete in the tension–compression region, while adding steel fibers to the mix of concrete increases its biaxial strength. Moreover, the biaxial failure criteria of UHSFC seem to be similar to those of normal-strength concrete, following the Kupfer's failure criteria.

4. A thorough interpretation of experimental results from previous works of Tsonos [38,39] was performed herein. The predictions of the proposed analytical methodology for the seismic performance of the retrofitted beam-column joint sub-assemblages were verified by the test results. Furthermore, the model satisfactorily predicted the failure mode of the strengthened specimens, which, in all cases, included the concentration of damage and the formation of plastic hinges solely in the beam of the specimens while the joint region and the columns remained intact. This is owed to the low actual shear stress values in the joint region which were lower than half the ultimate joint shear capacity ($\tau_{cal} < 0.5 \cdot \tau_{ult}$).
5. Common existing RC frames of civil infrastructures with under-reinforced beam-column connections require a sustainable and easy-to-apply strengthening technique to extend their service life. Conventional RC jackets and FRP wraps requires labor-intensive procedures and exhibit various shortcomings and constructional limitations. Application of HSFC or UHSFC jacketing provides a substantial increase to the shear capacity of beam-column joints along with feasibility, low cost and simplicity.
6. The proposed analytical methodology is feasible and provides accurate and reliable prediction of the hysteresis performance of retrofitted RC structures with innovative cost-effective HSFC and UHSFC jackets with various fraction ratios and without additional conventional reinforcement.

Author Contributions: Conceptualization, A.-D.T.; methodology, A.-D.T. and G.K.; software, G.K.; validation, A.-D.T. and G.K.; formal analysis, A.-D.T. and G.K.; investigation, A.-D.T.; resources, A.-D.T. and G.K.; data curation, G.K.; writing—original draft preparation, G.K.; writing—review and editing, A.-D.T.; visualization, A.-D.T. and G.K.; supervision, A.-D.T. All authors have read and agreed to the published version of the manuscript.

Funding: This research received no external funding.

Institutional Review Board Statement: Not applicable.

Informed Consent Statement: Not applicable.

Data Availability Statement: Not applicable.

Conflicts of Interest: The authors declare no conflict of interest.

Abbreviations

RC	Reinforced concrete
SFC	Steel fiber-reinforced concrete
HSFC	High-strength steel fiber-reinforced concrete
UHSFC	Ultra-high strength steel fiber-reinforced concrete

References

1. Tsonos, A.-D. Effectiveness of CFRP-jackets and RC-Jackets in post-earthquake and pre-earthquake retrofitting of beam–column subassemblages. *Eng. Struct.* **2008**, *30*, 777–793. [CrossRef]
2. Tsonos, A.-D. Ultra-high-performance fiber reinforced concrete: An innovative solution for strengthening old R/C structures and for improving the FRP strengthening method. *WIT Trans. Eng. Sci.* **2009**, *64*, 12.
3. Golias, E.; Zapris, A.; Kytinou, V.; Kalogeropoulos, G.; Chalioris, C.; Karayannis, C. Effectiveness of the novel rehabilitation method of seismically damaged RC joints using C-FRP ropes and comparison with widely applied method using C-FRP sheets—Experimental investigation. *Sustainability* **2021**, *13*, 6454. [CrossRef]
4. Kalogeropoulos, G.; Tsonos, A.-D.; Konstandinidis, D.; Tsetines, S. Pre-earthquake and post-earthquake retrofitting of poorly detailed exterior RC beam-to-column joints. *Eng. Struct.* **2016**, *109*, 1–15. [CrossRef]
5. Golias, E.; Zapris, A.; Kytinou, V.; Oscan, M.; Koumtzis, M.; Sapiera, D.; Chalioris, C.; Karayannis, C. Application of X-shaped CFRP ropes for structural upgrading of reinforced concrete beam-column joints under cyclic loading—Experimental study. *Fibers* **2021**, *9*, 42. [CrossRef]
6. Chalioris, C.E.; Zapris, A.G.; Karayannis, C.G. U-jacketing applications of fiber-reinforced polymers in reinforced concrete T-beams against shear—Tests and design. *Fibers* **2020**, *8*, 13. [CrossRef]

7. Tsonos, A.-D. Lateral load response of strengthened reinforced concrete beam-to-column joints. *ACI Struct. J. Proc.* **1999**, *96*, 46–56.
8. Paulay, T.; Park, R. *Joints of Reinforced Concrete Frames Designed for Earthquake Resistance*; Research Report No. 84-9; Department of Civil Engineering, University of Canterbury: Christchurch, New Zealand, 1984.
9. Karayannis, C.; Chalioris, C.; Sideris, K. Effectiveness of R/C beam-column connection repair using epoxy resin injections. *J. Earthq. Eng.* **1998**, *2*, 217–240. [CrossRef]
10. Park, R. A summary of results of simulated seismic load tests on reinforced concrete beam-column joints, beams and columns with substandard reinforcing details. *J. Earthq. Eng.* **2000**, *6*, 147–174. [CrossRef]
11. Karayannis, C.G.; Favvata, M.J.; Kakaletsis, D. Seismic behavior of infilled and pilotis RC frame structures with beam-column joint degradation effect. *Eng. Struct.* **2011**, *33*, 2821–2831. [CrossRef]
12. Karayannis, C. Mechanics of external RC beam-column joints with rectangular spiral shear reinforcement: Experimental verification. *Meccanica* **2015**, *50*, 311–322. [CrossRef]
13. Pampanin, S.; Calvi, G.M.; Moratti, M. Seismic behaviour of R.C. beam-column joints designed for gravity loads. In Proceedings of the 12th European Conference on Earthquake Engineering, London, UK, 9–13 September 2002.
14. Pampanin, S.; Bolognini, D.; Pavese, A. Performance-based seismic retrofit strategy for existing reinforced concrete frame systems using fiber-reinforced polymer composites. *J. Compos. Constr.* **2007**, *11*, 211–226. [CrossRef]
15. Chalioris, C.; Bantilas, K. Shear strength of reinforced concrete beam-column joints with crossed inclined bars. *Eng. Struct.* **2017**, *140*, 241–255. [CrossRef]
16. Kakaletsis, D.; David, K.; Karayannis, C. Effectiveness of some conventional seismic retrofitting techniques for bare and infilled R/C frame. *Struct. Eng. Mech.* **2011**, *39*, 499–520. [CrossRef]
17. Karayannis, C.; Chalioris, C.; Sirkelis, G. Local retrofit of exterior RC beam-column joints using thin RC jackets—An experimental study. *Earthq. Eng. Struct. D* **2008**, *37*, 727–740. [CrossRef]
18. Rodriguez, M.; Santiago, S. Simulated seismic load tests on two-storey waffle-flat-plate structure rehabilitated by jacketing. *ACI Struct. J.* **1998**, *95*, 129–145.
19. Tsonos, A.-D. Seismic repair of exterior R/C beam-to-column joints using two-sided and three-sided jackets. *Struct. Eng. Mech.* **2002**, *13*, 17–34. [CrossRef]
20. Tsonos, G.-D. Performance enhancement of R/C building columns through shotcrete jacketing. *Eng. Struct.* **2010**, *32*, 726–740. [CrossRef]
21. United Nations Industrial Development Organization (UNIDO). Repair and strengthening of reinforced concrete, stone and brick masonry buildings. In *Building Construction under Seismic Conditions in the Balkan Regions*; UNDP/UNIDO Project RER/79/015; United Nations Industrial Development Organization: Vienna, Austria, 1983; 231p.
22. Chalioris, C.E.; Kytinou, V.K.; Voutetaki, M.E.; Papadopoulos, N.A. Repair of heavily damaged RC beams failing in shear using U-shaped mortar jackets. *Buildings* **2019**, *9*, 146. [CrossRef]
23. Chalioris, C.E.; Pourzitidis, C.N. Rehabilitation of shear-damaged reinforced concrete beams using self-compacting concrete jacketing. *Int. Sch. Res. Not.* **2012**, *2012*, 816107. [CrossRef]
24. Karayannis, G.C.; Sirkelis, M.G. Strengthening and rehabilitation of RC beam-column joints using carbon-FRP jacketing and epoxy resin injection. *Earthq. Eng. Struct. D* **2008**, *37*, 769–790. [CrossRef]
25. Henager, C.H. *Steel Fibrous Ductile Concrete Joints for Seismic-Resistant Structures. Reinforced Concrete Structures in Seismic Zone*; ACI Special Publication, SP-53; American Concrete Institute: Detroit, MI, USA, 1977; pp. 371–386.
26. Chalioris, C.E.; Sfiri, E.F. Shear performance of steel fibrous concrete beams. *Procedia Eng.* **2011**, *14*, 2064–2068. [CrossRef]
27. Chalioris, C.E. Steel fibrous RC beams subjected to cyclic deformations under predominant shear. *Eng. Struct.* **2013**, *49*, 104–118. [CrossRef]
28. Chalioris, C.E.; Panagiotopoulos, T.A. Flexural analysis of steel fibre-reinforced concrete members. *Comput. Concr.* **2018**, *22*, 11–25.
29. Brandt, A.M. Fibre reinforced cement-based (FRC) composites after over 40 years of development in building and civil engineering. *Comp. Struct.* **2008**, *86*, 3–9. [CrossRef]
30. Marcalikova, Z.; Cajka, R.; Bilek, V.; Bujdos, D.; Sucharda, O. Determination of mechanical characteristics for fiber-reinforced concrete with straight and hooked fibers. *Crystals* **2020**, *10*, 545. [CrossRef]
31. Cajka, R.; Marcalikova, Z. Experimental tests of fiber-reinforced concrete slabs and comparison of deformations using 3D graphs. *Civ. Envir. Eng.* **2021**, *17*, 96–106.
32. Čajka, R.; Maňásek, P. Finite element analysis of a structure with a sliding joint affected by deformation loading. In Proceedings of the 11th International Conference on Civil, Structural and Environmental Engineering Computing, St. Julians, Malta, 18–21 September 2007; Civil-Comp Press: Stirlingshire, UK, 2007.
33. Cajka, R.; Marcalikova, Z.; Bilek, V.; Sucharda, O. Numerical modeling and analysis of concrete slabs in interaction with subsoil. *Sustainability* **2020**, *12*, 9868. [CrossRef]
34. Tsonos, A.-D.; Kalogeropoulos, G.; Iakovidis, P.; Konstantinidis, D. Seismic retrofitting of pre-1970 RC bridge columns using innovative jackets. *Int. J. Struct. Eng.* **2017**, *8*, 133–147. [CrossRef]
35. Kalogeropoulos, G.; Tsonos, A.-D.; Konstantinidis, D.; Iakovidis, P. Earthquake-resistant rehabilitation of existing RC structures using high-strength steel fiber-reinforced concrete jackets. *Earthq. Struct.* **2019**, *17*, 115–129.
36. Hackman, L.; Farell, M.; Dunhan, O. Slurry infiltrated mat concrete (SIMCON). *Concr. Int.* **1992**, *14*, 53–56.

37. Dogan, E.; Krstulovic-Opara, N. Seismic retrofit with continuous slurry-infiltrated mat concrete jackets. *ACI Struct. J.* **2003**, *100*, 713–722.
38. Tsonos, A.-D. A new method for earthquake strengthening of old R/C structures without the use of conventional reinforcement. *Struct. Eng. Mech.* **2014**, *52*, 391–403. [CrossRef]
39. Tsonos, A.-D. An innovative solution for strengthening of R/C structures and for improving the FRP strengthening method. *Struct Monit. Maint.* **2014**, *1*, 323–338. [CrossRef]
40. Tsonos, A.-D. Steel fiber reinforced concrete of high-strength for the construction of jackets for earthquake-strengthening of buildings without the use of conventional reinforcement. Patent 1005657; awarded by the Greek Industrial Property Organization (OBI), 2007.
41. Tsonos, A.-D. Cyclic load behaviour of reinforced concrete beam-column subassemblages of modern structures. *ACI Struct. J.* **2007**, *194*, 468–478.
42. Tsonos, A.-D.; Kalogeropoulos, G.; Iakovidis, P.; Bezas, M.-Z.; Koumtzis, M. Seismic performance of RC beam-column joints designed according to older and modern codes: An attempt to reduce conventional reinforcement using steel fiber reinforced concrete. *Fibers* **2021**, *9*, 45. [CrossRef]
43. Tsonos, A.-D. Model for the evaluation of the beam-column joint ultimate strength—A more simplified version. *Earthq. Struct.* **2019**, *16*, 141–148.
44. Parker, D.E.; Bullman, P.J.M. Shear strength within reinforced concrete beam–column joints. *Struct. Eng.* **1997**, *75*, 53–57.
45. Kaku, T.; Asakusa, H. Ductility estimation of exterior beam–column subassemblages in reinforced concrete frames. *ACI Struct. J. Spec. Publ.* **1991**, *123*, 167–186.
46. Uzumeri, S.M. Strength and ductility of cast-in-place beam–column joints. In *Reinforced Concrete Structures in Seismic Zones Publication*; ACI SP 53–12; The National Academies of Sciences, Engineering, and Medicine: Washington, DC, USA, 1997; pp. 293–350.
47. El-Nabawy Atta, A.; El-Din Fahmy Taher, S.; Khalil, A.-H.A.; El-Metwally, S.E. Behaviour of reinforced high-strength concrete beam—Column joint. Part II: Numerical simulation. *Struct. Conc.* **2004**, *5*, 101–112. [CrossRef]
48. Park, S.; Mosalam, K.M. *Shear Strength Models of Exterior Beam—Column Joints without Transverse Reinforcement*; PEER 2009/106; Pacific Earthquake Engineering Research Center, University of California: Berkeley, CA, USA, 2009; 87p.
49. Moehle, J.P.; Hassan, W.M. Experimental and analytical assessment of seismic vulnerability of exterior corner beam—Column joints in existing gravity RC buildings. In *NEES Grand Challenge Project: Mitigation of Collapse Risk in Older Concrete Buildings*; University of California: Berkeley, CA, USA, 2010.
50. Sharma, A.; Eligehausen, R.; Reddy, G.R. A new model to simulate joint shear behavior of poorly detailed beam—Column connections in RC structures under loads, part IQ exterior joints. *J. Eng. Struct.* **2011**, *33*, 1034–1051. [CrossRef]
51. Bakir, P.G. Seismic resistance and mechanical behavior of exterior beam-column joints with crossed inclined bars. *Struct. Eng. Mech.* **2003**, *16*, 493–517. [CrossRef]
52. European Committee for Standardization. *Eurocode 8: Design of Structures for Earthquake Resistance. Part 1: General Rules, Seismic Actions and Rules for Buildings*; EN 1998-1; European Committee for Standardization: Brussels, Belgium, 2004; 229p.
53. Park, R.; Paulay, T. *Reinforced Concrete Structures*; John Wiley Publications: New York, NY, USA, 1975.
54. Scott, B.D.; Park, R.; Priestley, M.J.N. Stress-strain behavior of concrete confined by overlapping hoops at low and high strain rates. *ACI J. Proc.* **1982**, *79*, 13–27.
55. Mohamed, R.N.; Zamri, N.F.; Elliott, K.S.; Rahman, A.B.A.; Bakhary, N. Steel fibre self-compacting concrete under biaxial loading. *Constr. Build. Mat.* **2019**, *224*, 255–265. [CrossRef]
56. Swanepoel, W. The Behaviour of Fibre Reinforced Concrete (SHCC) under Biaxial Compression and Tension. Master's Thesis, University of Stellenbosch, Stellenbosch, South Africa, December 2011; p. 134.
57. Van Dear Aa, P.J. Biaxial Stresses in Steel Fibre Reinforced Concrete Modeling the Pull Out-Behaviour of a Single Steel Fibre Using FEM. Master's Thesis, Eindhoven University of Technology, Eindhoven, The Netherlands, 2014; p. 133.
58. Kölle, B.; Phillips, D.V.; Zhang, B.; Bhatt, P.; Pearce, C.J. Experimental investigation of the biaxial properties of high performance steel fibre reinforced concrete. In Proceedings of the 6th Symposium on Fibre-Reinforced Concretes (FRC)—BEFIB 2004, Varenna, Italy, 20–22 September 2004; pp. 369–378.
59. Kölle, B. Behaviour of Steel Fibre Reinforced High Performance Concrete under Biaxial Loading Conditions. Ph.D. Thesis, University of Glasgow, Glasgow, UK, 2006; p. 319.
60. Chiew, S.M.; Ibrahim, I.S.; Sarbini, N.N.; Mohamed, R.N.; Jamaluddin, N. Behaviour of plain concrete and steel fibre reinforced concrete (SFRC) under biaxial stress—A review. *IOP Conf. Ser. Mater. Sci. Eng.* **2018**, *431*, 042006. [CrossRef]
61. Tschegg, E.K. Biaxial fracture behaviour of steel-span and steel-fibre-reinforced concrete. *J. Adv. Conc. Tech.* **2009**, *7*, 229–238. [CrossRef]
62. Tschegg, E.K.; Schneemayer, A.; Merta, I.; Rieder, K.A. Energy dissipation capacity of fibre reinforced concrete under biaxial tension—Compression load. Part II: Determination of the fracture process zone with the acoustic emission technique. *Cement Conc. Comp.* **2015**, *62*, 187–194. [CrossRef]
63. Marì Bernat, A.; Spinella, N.; Recupero, A.; Cladera, A. Mechanical model for the shear strength of steel fiber reinforced concrete (SFRC) beams without stirrups. *Mat. Struct.* **2020**, *53*, 28. [CrossRef]

64. Pasa Dutra, V.F.; Maghous, S.; Campos Filho, A. Micro mechanical approach to strength properties of steel fiber reinforced concrete. In Proceedings of the IV International Symposium on Solid Mechanics—MecSol, Porto Alegre, Brazil, 18–19 April 2013.
65. Lee, J.-H.; Hong, S.-G.; Joh, I.K.; Lee, J.-W. Biaxial tension-compression strength behaviour of UHPFRC in-plane elements. *Mat. Struct.* **2017**, *50*, 20. [CrossRef]
66. Kupfer, H.; Hilsdorf, H.K.; Rusch, H. Behavior of concrete under biaxial stresses. *ACI J.* **1969**, *66*, 656–667.
67. Feeling, E.; Leutbecher, T.; Roeder, F.-K. Compression—Tension strength of reinforced and fiber-reinforced concrete. *ACI Struct. J.* **2011**, *108*, 350–359.